



Iron assimilation by the clam *Laternula elliptica*: Do stable isotopes ($\delta^{56}\text{Fe}$) help to decipher the sources?



Harald Poigner^{a,*}, Dorothee Wilhelms-Dick^a, Doris Abele^{a,*}, Michael Staubwasser^b, Susann Henkel^{a,b}

^a Alfred Wegener Institute Helmholtz Centre for Polar and Marine Research, 27570 Bremerhaven, Germany

^b University of Cologne, Institute for Geology and Mineralogy, 50674 Cologne, Germany

HIGHLIGHTS

- The $\delta^{56}\text{Fe}$ fingerprint in hemolymph of *Laternula elliptica* was determined.
- At both stations hemolymph $\delta^{56}\text{Fe}$ values were highly variable among animals.
- Mean $\delta^{56}\text{Fe}$ values are lighter (0.5–0.85‰) than the reactive Fe of the sediment.
- This agrees with the preferential assimilation of light isotopes from nutrition.
- High variability in hemolymph $\delta^{56}\text{Fe}$ signatures limits $\delta^{56}\text{Fe}$ values as tracer.

ARTICLE INFO

Article history:

Received 2 June 2014

Received in revised form 15 April 2015

Accepted 25 April 2015

Keywords:

Iron
Stable isotopes
Hemolymph
Bivalve
Antarctica

ABSTRACT

Iron stable isotope signatures ($\delta^{56}\text{Fe}$) in hemolymph (bivalve blood) of the Antarctic bivalve *Laternula elliptica* were analyzed by Multiple Collector-Inductively Coupled Plasma-Mass Spectrometry (MC-ICP-MS) to test whether the isotopic fingerprint can be tracked back to the predominant sources of the assimilated Fe. An earlier investigation of Fe concentrations in *L. elliptica* hemolymph suggested that an assimilation of reactive and bioavailable Fe (oxyhydr)oxide particles (i.e. ferrihydrite), precipitated from pore water Fe around the benthic boundary, is responsible for the high Fe concentration in *L. elliptica* (Poigner et al., 2013b).

At two stations in Potter Cove (King George Island, Antarctica) bivalve hemolymph showed mean $\delta^{56}\text{Fe}$ values of $-1.19 \pm 0.34\text{‰}$ and $-1.04 \pm 0.39\text{‰}$, respectively, which is between 0.5‰ and 0.85‰ lighter than the pool of easily reducible Fe (oxyhydr)oxides of the surface sediments (-0.3‰ to -0.6‰). This is in agreement with the enrichment of lighter Fe isotopes at higher trophic levels, resulting from the preferential assimilation of light isotopes from nutrition. Nevertheless, $\delta^{56}\text{Fe}$ hemolymph values from both stations showed a high variability, ranging between -0.21‰ (value close to unaltered/primary Fe(oxyhydr)oxide minerals) and -1.91‰ (typical for pore water Fe or diagenetic Fe precipitates), which we interpret as a “mixed” $\delta^{56}\text{Fe}$ signature caused by Fe assimilation from different sources with varying Fe contents and $\delta^{56}\text{Fe}$ values. Furthermore, mass dependent Fe fractionation related to physiological processes within the bivalve cannot be ruled out.

This is the first study addressing the potential of Fe isotopes for tracing back food sources of bivalves.

© 2015 Published by Elsevier Ltd.

1. Introduction

Benthic deposit feeders ingest particles and water from the benthic boundary layer and assimilate trace metals dissolved in seawater, bottom water, and pore water, as well as bound or adsorbed to organic and lithogenic particles (Rainbow, 2002;

Griscom and Fisher, 2004). Dominating assimilation pathways and bioavailable metal sources are difficult to track. This would, however, be important to understand environmental impact, including sources of contamination in marine bivalve populations, and also the biogeochemical processes that render environmental metals/contaminants as “bioavailable”. Tissue specific Fe-contents in the circum-Antarctic clam *Laternula elliptica* (King and Broderip, 1832) vary considerably between sampling sites around the Antarctic continent (Ahn et al., 1996; Nigro et al., 1997; Lohan et al., 2001; Deheyn et al., 2005; Curtosi et al., 2010; Husmann

* Corresponding authors.

E-mail addresses: Harald.Poigner@awi.de (H. Poigner), Doris.Abele@awi.de (D. Abele).

et al., 2012; Poigner et al., 2013b). Highest contents were found at Deception Island where hydrothermal waters release high loads of dissolved Fe into the environment (Rey et al., 1995; Deheyn et al., 2005). At King George Island (KGI; Isla 25 de Mayo) the predominant source for Fe assimilation in *L. elliptica* remains unclear and has been controversially discussed in recent papers. Several authors assumed lithogenic sediment particles derived by sedimentation of glacial debris to be the source for high Fe tissue contents in the Antarctic clam (e.g. Abele et al., 2008; Curtosi et al., 2010; Husmann et al., 2012). Alternatively, Poigner et al. (2013b) propose bioavailable Fe (oxyhydr)oxides, in particular ferrihydrite that precipitates from sediment pore water Fe^{2+} , as predominant Fe source for *L. elliptica* in Potter Cove. This argumentation highlights the fast oxidation of dissolved inorganic Fe^{2+} in the pore water to Fe^{3+} , as soon as it reaches nitrate-containing pore water,oxic sediment layers or bottom water (Ahrland, 1975; Kasten et al., 2004). Iron(III) is affected by strong hydrolysis and precipitates as nanoparticulate Fe(oxyhydr)oxides (Ahrland, 1975; Millero et al., 1995; Waite, 2001), particularly as metastable ferrihydrite ($\text{Fe}_4\text{HO}_8 \cdot 4\text{H}_2\text{O}$, earlier specified as $\text{Fe}(\text{OH})_3$; reviewed in Raiswell and Canfield, 2012), which is characterized by a high solubility and reactivity and, thus, is highly bioavailable (Raiswell and Canfield, 2012).

The stable Fe isotope signature of *L. elliptica* hemolymph may be suitable to trace back the predominant environmental Fe source. Iron isotope analysis is emerging as a tracer for biogeochemical Fe cycling in aquatic environments (Anbar and Rouxel, 2007) as post-sedimentary precipitated Fe (oxyhydr)oxides as well as pore water Fe^{2+} are known to be significantly enriched in light Fe isotopes compared to terrigenous Fe minerals (Severmann et al., 2006; Staubwasser et al., 2006, 2013).

Stable Fe isotopes occur in the following relative abundances: ^{54}Fe : 5.84%, ^{56}Fe : 91.76%, ^{57}Fe : 2.12%, and ^{58}Fe : 0.28% (Taylor et al., 1992). The terminology and general isotopic fractionation reactions have been reviewed by Anbar (2004). In brief, Fe isotopic compositions are commonly expressed as $^{56}\text{Fe}/^{54}\text{Fe}$ and $^{57}\text{Fe}/^{54}\text{Fe}$ ratios, whereas the δ notation is widely used to demonstrate isotopic shifts of samples against a standard material. The $\delta^{56}\text{Fe}$ value [‰] relates the $^{56}\text{Fe}/^{54}\text{Fe}$ ratio of a sample to the $^{56}\text{Fe}/^{54}\text{Fe}$ ratio of the standard reference material IRMM-014 (Eq. (1)).

$$\delta^{56}\text{Fe}[\text{‰}] = \left(\frac{(^{56}\text{Fe}/^{54}\text{Fe})_{\text{Sample}}}{(^{56}\text{Fe}/^{54}\text{Fe})_{\text{IRMM-014}}} - 1 \right) \times 1000 \quad (1)$$

Shifts in $\delta^{56}\text{Fe}$ values result from mass dependent fractionation during biotic and abiotic processes. During early diagenetic reactions in the sediments, which are fueled by microbial degradation of organic matter, Fe isotopes become fractionated between different reactive Fe mineral phases – essentially most non Si-bound Fe minerals, such as (oxyhydr)oxides and sulfides – and between reactive Fe minerals and dissolved Fe species (Beard and Johnson, 2004). For instance, the oxidation of electron donors and reduction of a metal used by microbes to obtain energy, namely microbial dissimilatory iron reduction (DIR), preferentially releases light Fe isotopes into solution (e.g., Beard et al., 1999, 2003; Crosby et al., 2007). This process results in negative $\delta^{56}\text{Fe}$ values of pore water Fe^{2+} , whereas the sedimentary Fe residual shows progressively higher $\delta^{56}\text{Fe}$ values with sediment depth (Severmann et al., 2006; Staubwasser et al., 2006). In contrast, sulfide precipitation results in higher $\delta^{56}\text{Fe}$ pore water values due to the preferential precipitation of light Fe isotopes (Severmann et al., 2006). This fractionation pattern dominates sediment layers where hydrogen sulfide (HS^-) originating from organoclastic sulfate reduction or anaerobic oxidation of methane and Fe^{2+} counter-diffuse (compare Kasten et al., 2004). Hence, $\delta^{56}\text{Fe}$ signatures of pore water range widely between +0.5‰ and –4.0‰ depending on the isotopic composition

of reactive Fe minerals deposited on the sea floor and the degree/extent of early diagenetic processes (e.g., Bergquist and Boyle, 2006; Staubwasser et al., 2006; Severmann et al., 2006, 2010; Homoky et al., 2009). In consequence, the isotopic Fe signatures of the described Fe sources, which are ingested by *L. elliptica*, are expected to vary. Important Fe sources in Potter Cove in particular include eroded bedrock material from the adjacent peninsula, dissolved pore water Fe^{2+} , and precipitated Fe (oxyhydr)oxides. Further nanoparticulate Fe (oxyhydr)oxides can also be released into coastal waters or sediments by deglaciation (Raiswell et al., 2006, 2008; Monien et al., 2013).

Trace metal concentrations (e.g., Fe) in the bivalve hemolymph represent the product of cutaneous (gills) and intestinal (digestive tract) assimilation, and the compartmentalization into several tissues with varying metal turnover rates (George et al., 1976; Simkiss and Taylor, 1981; Simkiss and Mason, 1983). Hence, hemolymph is not only regarded as the organ of first storage but, due to the subsequent binding of Fe ions to organic ligands (e.g., enzymes and other proteins; Simkiss and Mason, 1983; Gonzalez et al., 2010; Gonzalez and Puntarulo, 2011), it is further of particular importance for the metal transport from assimilation sites to sites of excretion (Simkiss and Mason, 1983; Kadar et al., 2010). However, a few studies found a linear relationship of Fe concentrations in hemolymph of *L. elliptica* (Poigner et al., 2013b) and tissues of *Mytilus edulis* (George et al., 1976; George and Coombs, 1977) to experimentally adjusted Fe concentrations (particulate and/or dissolved). Here, for the first time, $\delta^{56}\text{Fe}$ values of the hemolymph of the Antarctic clam *L. elliptica* are reported and discussed based on known Fe fractionation patterns in subsurface sediments. Since the Fe isotope signature of the hemolymph may reflect the isotopic fingerprint of the assimilation source, we compare isotopic Fe signatures among bivalve hemolymph and environmental Fe sources, in particular sediment and pore water data found in the literature, to assess the predominating Fe source for *L. elliptica* in Potter Cove.

2. Material and methods

Individuals of the Antarctic soft shell clam *L. elliptica* and sediment cores for pore water extraction were collected at two stations in Potter Cove on King George Island (Fig. 1) between January and March 2012. Potter Cove is covered by the Universal Transverse Mercator (UTM) grid zone Z21E (WGS84). STA04 is located at 0414281 E and 3098994 N (water depth: 12 m) and STA11 at 0413179 E and 3098287 N (water depth: 6 m). Bivalves as well as the core at site STA11, were sampled by scuba divers, whereas the sediment core at site STA04 was gained using an UWITEC gravity corer.

Pore water was extracted immediately after retrieving the cores using rhizon samplers with a mean pore size of 0.15 μm (Seeberg-Elverfeldt et al., 2005; Dickens et al., 2007). Aliquots of pore water were taken for SO_4^{2-} and dissolved iron (Fe^{2+}) analyses. For photometric analysis of Fe^{2+} , 1 mL sample aliquots were transferred into cuvettes pre-filled with a 50 μL Ferrospectral solution. At high Fe^{2+} concentrations ($>1 \text{ mg L}^{-1}$), sample aliquots were preserved with 10 μL of 1% ascorbic acid and subsequently diluted with oxygen-free artificial seawater. Analyses of Fe^{2+} were performed using a CECIL CE2021 photometer at a wavelength of 565 nm. Sulfate measurements were performed at the Alfred Wegener Institute by suppressed ion chromatography at a 1:50 dilution with 18 M Ω -water on a Metrohm IC Net 2.3. Seawater provided by the International Association for the Physical Sciences of the Oceans (IAPSO) was used in each run either for preparation of the calibration standards or as a quality control.

Hemolymph (fluid and hemocyte cells) was taken of the posterior adductor muscle using a G26x1 needle (Sterican[®], B. Braun

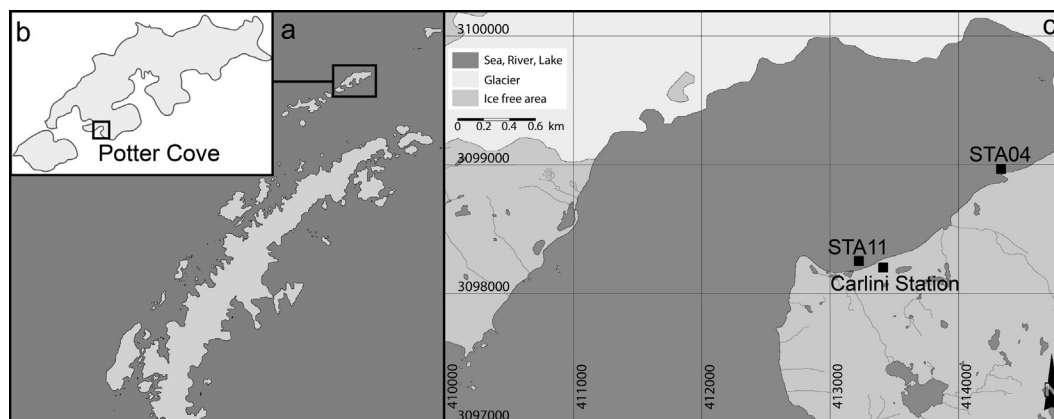


Fig. 1. (a) Map of the Antarctic Peninsula (King George Island highlighted), (b) Map of King George Island, (c) Map of Potter Cove including the sampling stations (UTM grid; zone Z21E; WGS84).

Melsungen AG, Germany) and a 1 mL syringe (Omnifix[®], B. Braun Melsungen AG, Germany) within 12 h after collecting the clams. This stainless Cr–Ni–steel needle is coated by a thin silicone film. So Fe contamination due to the contact of blood and the steel surface is prevented. Samples were acidified with 100 μ L nitric acid (65%, suprapure quality) per 1.5 mL hemolymph and stored and transported at 4 °C.

Prior to hydrolysis all beakers (PTFE, PFA) were first cleaned with acetone, then with 3 M HCl (p.a. grade) at 120 °C (>6 h), afterwards with 7.5 M HNO₃ (p.a. grade) at 120 °C (>6 h), and finally with deionized water at 100 °C (>6 h). All other vials and tubes (PP, PE) were cleaned with 3% alkaline detergent (24 h) and subsequently with 3 M HCl (3 days; p.a. grade) at room temperature. Additionally, PP vials were left in 7.5 M HNO₃ (p.a. grade) for 6 h. After the cleaning procedure beakers and vials were rinsed with deionized water first and finally with 18.2 M Ω -water.

Hemolymph (1–1.5 mL) was transferred to PTFE beakers and sample vials were rinsed with 1 M bidistilled HNO₃ to ensure the complete transfer of the sample. First, 5 mL of HNO₃ (65%, sub-boiled) and 1 mL of H₂O₂ (30%, suprapure) were added to the beakers. Samples were kept at room temperature for 4 h to avoid strong outgassing. The beakers were then heated under stirring for 1 h at 60 °C, 1 h at 120 °C, and 8 h at 160 °C and thereafter evaporated at 160 °C. After cooling, the residuals were dissolved in 5 mL of 6 M HCl, evaporated at 90 °C, and redissolved in 6 M distilled HCl.

Chemical separation of Fe and subsequent analysis of stable Fe isotopes were performed at the University of Cologne and the Steinmann Institute in Bonn following established procedures (Schoenberg and von Blanckenburg, 2005). Iron was separated from other ions by anion-exchange chromatography using BioRad AG[®] 1-X8, 100–200 mesh resin in a 7.5 mL Spectrum[®] PP column to avoid potential matrix effects during Fe isotope analysis.

The Fe-containing fraction was evaporated at 90 °C and subsequently redissolved in 1 mL 0.3 M HNO₃ (dest.). Sample splits of 100 μ L were diluted to a final volume of 5 mL with 0.3 M HNO₃ (dest.) in order to determine Fe concentrations using Inductively Coupled Plasma–Optical Emission Spectroscopy (ICP–OES; Spectro Arcos, SPECTRO Analytical Instruments GmbH). Afterwards, the original purified Fe samples were diluted to a final concentration of 1 mg L⁻¹ Fe for final Fe isotope analyses by Multiple Collector–ICP–Mass Spectrometry (MC–ICP–MS, ThermoFinnigan Neptune). Iron isotope ratios were measured using the sample standard bracketing method. All $\delta^{56}\text{Fe}$ [‰] data are relative to the IRMM-14 standard reference material. A “JM” standard reference material (inhouse-standard) was measured ($N = 8$) in between

samples to check for precision and accuracy of the analyses and revealed an average $\delta^{56}\text{Fe}$ of 0.43 ± 0.02 ‰ (given value: 0.42 ± 0.05 ‰).

Hemolymph samples of *L. elliptica* contain high Zn concentrations (compare Poigner et al., 2013a). This potentially causes matrix effects during MC–ICP–MS analyses since the elution of Fe and Zn overlaps during anion-exchange chromatography and, thus, Zn is not completely removed (Schoenberg and von Blanckenburg, 2005). However, Fe standard solutions (Certipur[®], Merck, stock solution 1000 ppm) spiked with different Zn concentrations were measured to check for possible effects and were found to give similar results. The $\delta^{56}\text{Fe}$ values of Zn-spiked (1 and 2 mg L⁻¹ Zn) and non-spiked Fe standards did not differ significantly from each other (p -value: 0.153). Iron isotope data of measured hemolymph samples and JM standard reference material are plotted as $\delta^{57}\text{Fe}$ versus $\delta^{56}\text{Fe}$ in Fig. 2 to check the instrumental mass discrimination (Schoenberg and von Blanckenburg, 2005). The least-square regression through all samples features a slope of 1.50 ± 0.01 (adj. $R^2 = 0.997$) similar to the theoretical mass dependent fractionation line ($\delta^{57}\text{Fe} \approx 1.5 \times \delta^{56}\text{Fe}$). Further, it shows that the organic hemolymph matrix (i.e. organic molecules of the masses 54, 56, and 57) does not bias the Fe isotope analysis.

Descriptive statistics were computed in Origin 8.5.1 (OriginLab Corporation, USA). Differences in means were tested for significance between stations by the Welch-test and the two sample t -test (using R 2.12.1; R Development Core Team, 2010). Normal distribution and homogeneity of variances were tested by the Shapiro–Wilk-test and Bartlett’s test. An alpha level of 5% was chosen as statistically significant.

3. Results

At station STA04 hemolymph Fe concentrations (32 – 131 $\mu\text{mol L}^{-1}$ Fe) were within the range of pore water Fe²⁺ concentrations of the first 5 cm below seafloor (cmbfs; 5 – 120 $\mu\text{mol L}^{-1}$ Fe; Figs. 3 and 4). Station STA11 had Fe²⁺ pore water concentrations between 10 and 45 $\mu\text{mol L}^{-1}$ Fe within the upper 5 cm of the sediment column (Fig. 3), and Fe concentrations in hemolymph ranged between 28 and 186 $\mu\text{mol L}^{-1}$. Mean ($\pm 95\%$ confidence interval) Fe concentrations in hemolymph were 72 ± 20 $\mu\text{mol L}^{-1}$ (STA04, $N = 10$) and 89 ± 46 $\mu\text{mol L}^{-1}$ (STA11, $N = 9$) and did not differ significantly (p -value = 0.462) from station to station.

In bivalve hemolymph the $\delta^{56}\text{Fe}$ values ranged between -0.27 ‰ and -1.68 ‰ at STA11 and between -0.21 ‰ and -1.91 ‰ at STA04. Means did not deviate significantly

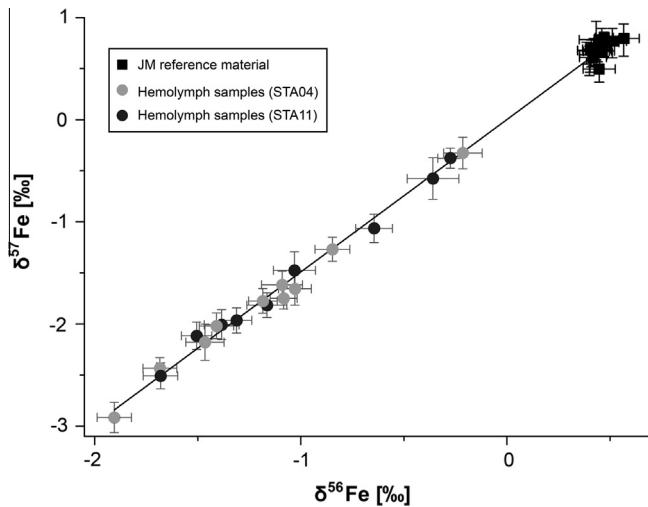


Fig. 2. Fe isotope data as $\delta^{57}\text{Fe}$ versus $\delta^{56}\text{Fe}$ of hemolymph samples of *L. elliptica* (solid circles; STA04: grey; STA11: black) and JM reference material (solid squares). Whiskers indicate the standard deviation. The regression line was determined by the least square method.

(p -value = 0.508) between both stations (STA04: $-1.19 \pm 0.34\text{‰}$, STA11: $-1.04 \pm 0.39\text{‰}$).

At both stations the SO_4^{2-} concentrations decrease only slightly with sediment depth (Fig. 4). Thus, the sulfate–methane transition zone (SMT) is located far below the cored sediment section.

4. Discussion

As a benthic deposit feeder *L. elliptica* inhales bottom and pore water and ingests organic and inorganic sediment particles from the benthic boundary layer. The contribution of Fe from these potential sources to the Fe assimilation of *L. elliptica* might vary regionally due to differing Fe contents and bioavailability. Further, the vertical redox zonation of the sediment exerts a strong influence on Fe cycling and Fe isotope fractionation. Hence, $\delta^{56}\text{Fe}$ signatures in both, sediment and pore water, vary with sediment depth (Severmann et al., 2006; Staubwasser et al., 2006).

In Potter Cove, dissolved Fe concentrations in pore water at both stations (STA04, STA11) peaked between 2 and 7 cm below seafloor (cmbsf), whereas high SO_4^{2-} concentrations were recorded throughout the cores. These profiles indicate that (i) the ferruginous zone, characterized by DIR and a release of dissolved Fe^{2+} from sediments into the pore water, is located between 2 and 10 cmbsf; (ii) only a thin sediment layer (1–2 cm) separates the ferruginous zone from the benthic boundary; and (iii) anaerobic oxidation of methane at the SMT takes place below the cored sediment section. The diminishment of pore water Fe^{2+} below ~ 6 cmbsf is likely due to the presence of hydrogen sulfide (HS^-) originating from organoclastic sulfate reduction or AOM at deeper depths according to the classical sequence of redox zones in marine sediments (Froelich et al., 1979; Berner, 1981; reviewed by Kasten et al., 2004). When sulfide and Fe^{2+} counter-diffuse, Fe sulfides precipitate potentially resulting in higher $\delta^{56}\text{Fe}$ pore water values at these depths compared to the benthic boundary (Severmann et al., 2006). The elevated pore water Fe^{2+} concentrations within the upper 10 cmbsf indicate a release of dissolved Fe^{2+} into the pore water as a result of DIR. The Fe diffusion gradients indicate that at shallow sediment depth close to the bivalve siphon (down to ~ 5 cmbsf), pore water and sediment $\delta^{56}\text{Fe}$ signatures are not affected by substantial Fe-sulfide precipitation.

In general, microbes favor light Fe isotopes during the reduction of Fe (oxyhydr)oxides. In consequence, the residual sediment

becomes relatively enriched in heavy Fe, whereas the pore water is characterized by low $\delta^{56}\text{Fe}$ values (Staubwasser et al., 2006). Dissolved Fe^{2+} diffuses upwards, precipitates as Fe (oxyhydr)oxide close to or within the thin oxic sediment layer or escapes into the water column via diffusion or bioturbative/irrigative fluxes (e.g., Slomp et al., 1997; Severmann et al., 2010). Bioirrigation and bioturbation might enhance the flux of dissolved Fe into the bottom water (Raiswell and Canfield, 2012). In contact with oxygen, kinetically constrained oxidative precipitation preferentially removes light Fe isotopes as Fe (oxyhydr)oxides (John et al., 2012; Staubwasser et al., 2013).

In Potter Cove, the reactive Fe fraction (leached by hydroxylamine–HCl following Poulton and Canfield, 2005) of surface sediments had $\delta^{56}\text{Fe}$ values of $-0.56 \pm 0.10\text{‰}$ and $-0.25 \pm 0.12\text{‰}$, respectively (S. Henkel, unpublished data from STA04 and a station at 0413719 E and 3099533 N), which is between 0.5‰ and 0.85‰ heavier than the mean $\delta^{56}\text{Fe}$ signature of bivalve hemolymph (-1.1‰ ; Fig. 3). Lighter Fe isotopes become enriched at higher trophic levels (Zhu et al., 2002) due to the preferential assimilation

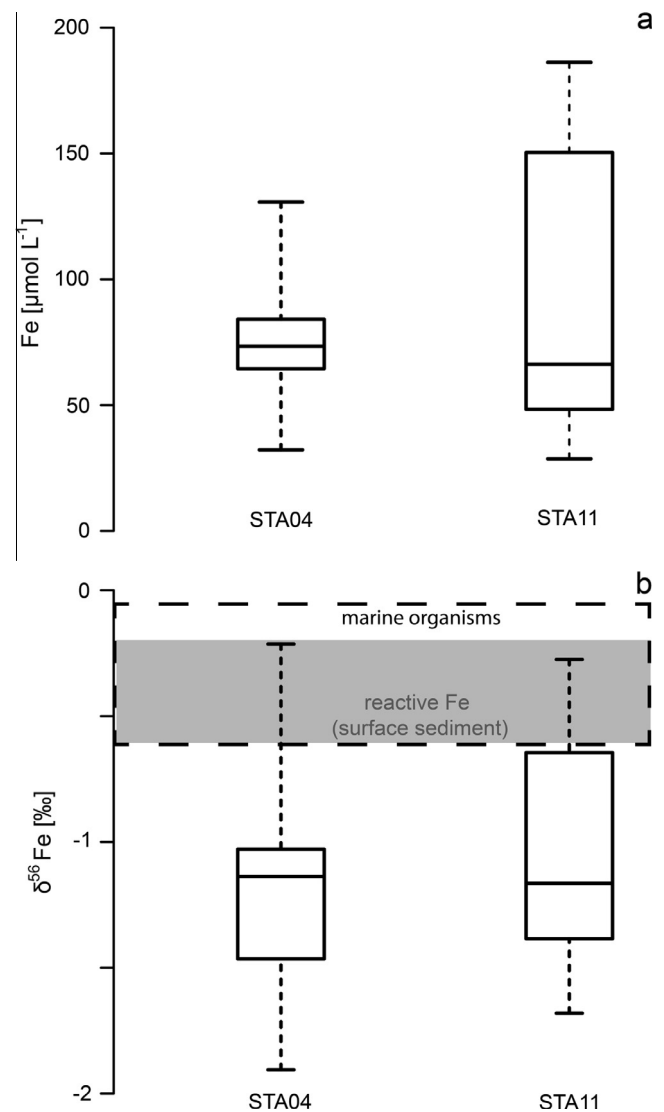


Fig. 3. Fe concentrations (a) and $\delta^{56}\text{Fe}$ (b) of bivalve hemolymph at STA04 ($N = 10$) and STA11 ($N = 9$). In (b) the grey solid area denotes the $\delta^{56}\text{Fe}$ range of the reactive (hydroxylamine–HCl leachable) Fe fraction in the surface sediment in Potter Cove (Henkel, unpubl.) and the black dashed frame highlights the range of $\delta^{56}\text{Fe}$ values of marine organisms from literature (Walczyk and von Blanckenburg, 2002; Bergquist and Boyle, 2006).

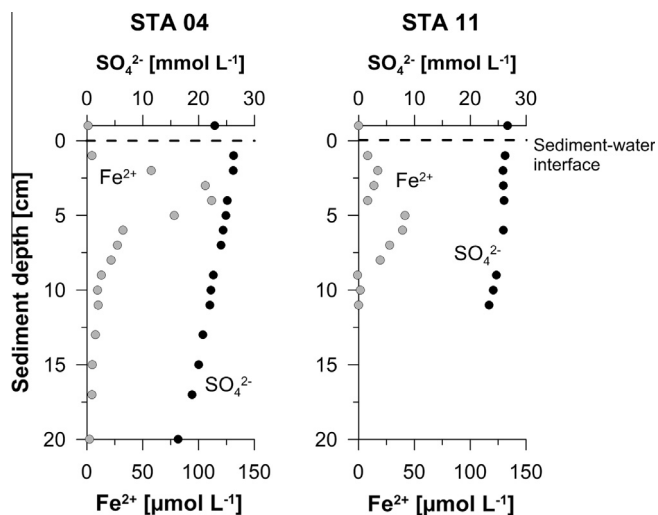


Fig. 4. Pore water profiles of Fe^{2+} and SO_4^{2-} of STA04 and STA11. Note the slightly lower SO_4^{2-} concentration in the bottom water at STA04, which is the result of high freshwater input by melt water streams in the vicinity of the station during low tide. The lower Fe^{2+} concentrations within the upper sediment layer and the break in Fe^{2+} concentrations at 5 cm sediment depth at STA11 are likely generated by a deeper oxygen penetration depth due to intense bioturbation at this site.

of light isotopes from dietary sources (e.g., humans: Walczyk and von Blanckenburg, 2002, 2005; mammals: Hotz et al., 2011; plants: Guelke and von Blanckenburg, 2007; Kiczka et al., 2010). Since *L. elliptica* occupies a low trophic position in the Antarctic food web (Norkko et al., 2007), we do not expect very low $\delta^{56}\text{Fe}$ signatures, except if the food of *L. elliptica* (i.e. benthic diatoms, detritus) is a priori depleted in $\delta^{56}\text{Fe}$. Hence, the low $\delta^{56}\text{Fe}$ hemolymph values suggest a Fe assimilation from ^{54}Fe -enriched reactive and bioavailable particles from the benthic boundary layer or pore water. Poigner et al. (2013b) proposed such particles as main Fe source for *L. elliptica* based on the high Fe concentrations in bivalve hemolymph and the fast response of Fe concentrations in hemolymph to environmental (bioavailable) Fe concentrations. (Note, that iron was provided experimentally as dissolved Fe:EDTA complex to ensure constant and reproducible conditions.) However, further Fe assimilation occurs from a wide spectrum of ingested (inorganic and organic) particles (compare Ahn, 1993; Norkko et al., 2007) and from inhaled pore water (e.g., if the siphon is retracted beneath the sediment surface or if pore water is advectively released due to bioturbation/irrigation). Although the proportion of assimilated Fe from these sources is assumed to be minor compared to the assimilation of Fe (oxyhydr)oxide particles (i.e., ferrihydrite; compare paragraph ii), it likely results in a mixed $\delta^{56}\text{Fe}$ fingerprint, which is expressed by the wide range of $\delta^{56}\text{Fe}$ values (-0.2‰ to -1.9‰) in hemolymph of animals from both stations (although mean $\delta^{56}\text{Fe}$ hemolymph values do not differ significantly among sites). Potential explanations, including the Fe assimilation from sources with different $\delta^{56}\text{Fe}$ signatures and Fe isotope fractionation related to transport and storage processes within the bivalve, are discussed in the following sections.

- (i) Pore water $\delta^{56}\text{Fe}$ values strongly depend on diagenetic processes and vary with sediment depth (Staubwasser et al., 2006). Close to the benthic boundary (sediment/water interface) pore water can probably be inhaled directly by the bivalve via the siphon, whereas pore water in deeper sediment layers, characterized by a different $\delta^{56}\text{Fe}$ value, can only reach the benthic boundary and/or the bivalve via bioturbation/irrigation. Hence, dissolved Fe^{2+} of different $\delta^{56}\text{Fe}$ signatures can reach the oxic sediment layer or the bottom

water and precipitate as Fe (oxyhydr)oxide (i.e. ferrihydrite). If the dissolved Fe^{2+} precipitates completely, the $\delta^{56}\text{Fe}$ signature of the precipitated Fe is identical to the pore water signature. Whereas, if dissolved Fe^{2+} precipitates partially, precipitated Fe will be isotopically lighter than the pore water signature due to the favored precipitation of lighter isotopes (Staubwasser et al., 2006, 2013).

Further, reactive and potentially bioavailable Fe (oxyhydr)oxides are also transported into Potter Cove via meltwater streams (Monien et al., 2013). Since lithogenic material remains relatively unfractionated during its transport by rivers (Beard et al., 2003), $\delta^{56}\text{Fe}$ values of $\sim 0\text{‰}$ are expected for these Fe particles, which may influence the isotopic Fe signature of bivalves in the vicinity of the meltwater inlets.

- (ii) Norkko et al. (2007) showed that the gut content of *L. elliptica* varies largely across sites and between seasons. In Potter Cove the composition of ingested particles was qualitatively analyzed on smear slides by means of light microscopy in March 2010 (Poigner, 2013). Lithogenic particles and fine detritus (organic and inorganic – visually undifferentiated) dominated in *L. elliptica* (material retrieved from siphon, gills, and digestive tract). Diatoms, mainly benthic (epipelagic) species of *Ceratoneis* spp. and *Pleurosigma* spp., and other organic particles (e.g., fragments of macroalgae, nematodes) occurred to a lesser extent (Poigner, 2013). However, $\delta^{56}\text{Fe}$ signatures of any potential organic food source (e.g., diatoms, macroalgae, detritus) for bivalves are lacking for Antarctica, but marine organisms of three different trophic levels from other regions showed $\delta^{56}\text{Fe}$ signatures clearly higher than -1‰ (mean $\delta^{56}\text{Fe}$ signature of *L. elliptica*: -1.1‰ ; Fig. 3).

Marine plankton from the Amazon shelf shows $\delta^{56}\text{Fe}$ values between -0.05‰ and -0.39‰ (mean: -0.24‰ ; Bergquist and Boyle, 2006) and two marine organisms of higher trophic levels had values of -0.2‰ (shrimp muscle) and -0.6‰ (tuna muscle; Walczyk and von Blanckenburg, 2002).

Since isotopic signatures of inorganic and organic bioavailable Fe can vary strongly, we expect inter-individual-differences in predominating Fe sources, total metabolic rate of an individual and relative proportion of each source compared to the total Fe assimilation to be mainly responsible for the variability of $\delta^{56}\text{Fe}$ hemolymph values among individuals from the same location (compare range in Fig. 3b).

- (iii) The $\delta^{56}\text{Fe}$ hemolymph signature can further be altered by mass dependent fractionation during physiological processes (assimilation, transport, storage) within the bivalve, as it was observed for Ca in the bivalve *Mytilus edulis* (Heinemann et al., 2008). Briefly, the extrapallial fluid (compartment of shell formation; $\delta^{44/40}\text{Ca} = -0.01\text{‰}$) was isotopically heavier than the Ca source, ambient seawater ($\delta^{44/40}\text{Ca} = -0.32\text{‰}$), due to a preferential incorporation of lighter Ca isotopes into the bivalve carbonate shell ($\delta^{44/40}\text{Ca} = -1.09\text{‰}$ to -1.33‰).

To date isotope fractionation during physiological processes related to Fe-assimilation, Fe-transport, and Fe-storage has only been intensively investigated with reference to humans (e.g., Walczyk and von Blanckenburg, 2002, 2005; Kraysenbuehl et al., 2005; Hotz et al., 2012; Hotz and Walczyk, 2013). Humans show the lightest Fe isotope signature among all investigated organisms which is due to the preferential assimilation of light isotopes from dietary sources ($\delta^{56}\text{Fe}$ values in human blood ranged between

–1.6‰ and –3.0‰; Walczyk and von Blanckenburg, 2002; Hotz et al., 2012). Nevertheless, Fe isotopic compositions of human blood vary between individuals due to differences in Fe metabolism (Walczyk and von Blanckenburg, 2002, 2005; Ohno et al., 2004; Hotz et al., 2011, 2012). Additionally, Ferritin-rich organs have heavier Fe isotope signatures, whereas red blood cells¹ are enriched in lighter isotopes (Walczyk and von Blanckenburg, 2002, 2005; Hotz et al., 2011, 2012). The low Fe turnover in humans explains why humans need months or years to restore the original isotopic blood composition (Hotz et al., 2012). Hence, isotope fractionation exerted by ferritin-based Fe storage mechanisms strongly affects the isotopic Fe signature of human blood (Hotz et al., 2012).

L. elliptica also expresses the Fe storage protein ferritin in several tissues (digestive gland, gill, foot) as well as in hemocyte cells in large quantities (Husmann, 2013). On average 30% of total Fe within the hemolymph¹ are bound in hemocyte cells (Poigner et al., 2013b) and digestive gland and gills show higher Fe contents (Husmann et al., 2012; Poigner et al., 2013a) compared to tissues of lower ferritin expression (e.g., siphon, mantle; liver was not investigated; Husmann et al., 2012; Husmann, 2013; Poigner et al., 2013a). Nevertheless, the Fe turnover is considerably faster in *L. elliptica* compared to humans, since Poigner et al. (2013b) found a drop of Fe concentrations in the hemolymph of ~50% within 15 days as soon as the animals were deprived of their environmental Fe source by exposure in Fe-free water.

Overall, we expect mass dependent fractionation related to the transfer of Fe into tissues and cells in *L. elliptica*. However, the sensitivity of the $\delta^{56}\text{Fe}$ hemolymph signature to such processes appears to be minor since Fe exhibits very high turnover rates in hemolymph of *L. elliptica*. Thus, $\delta^{56}\text{Fe}$ hemolymph values are likely more imprinted by the signature of “newly” assimilated Fe from the environment and fractionation during assimilation.

We conclude that all the processes we described here are expected to contribute to a mixed $\delta^{56}\text{Fe}$ fingerprint of bivalve hemolymph. However, so far we cannot determine to which extent. Thus, the $\delta^{56}\text{Fe}$ fingerprint in hemolymph of *L. elliptica* cannot yet be used as an accurate indicator to determine the predominant bioavailable Fe source. Nevertheless, we assume the Fe assimilation from reactive ferrihydrite particles to have the dominant imprint on the hemolymph signature. This conclusion is particularly based on (i) the fast response of hemolymph Fe concentrations to bioavailable environmental Fe concentrations (resulting in short half time values of Fe in *L. elliptica*; Poigner et al., 2013b), (ii) the high abundance of reactive (bioavailable), particulate Fe in Potter Cove (Henkel et al., 2013; Monien et al., 2013), and (iii) the conformity of averaged $\delta^{56}\text{Fe}$ values in bivalves hemolymph (–1.1‰) and the reactive Fe fraction in surface sediments (–0.25 ± 0.12‰ and –0.56 ± 0.10‰; S. Henkel, unpublished data) to the preferred assimilation of lighter isotopes along the food chain.

Acknowledgements

We would like to thank Stefanie Meyer (Alfred Wegener Institute for Polar and Marine Research, AWI) for her support during expedition preparations and Ilsetraut Stöltzing (AWI) for her help in the laboratories. Jan Hartmann (University of Heidelberg and AWI) is thanked for his support during sampling and analyzing of pore water samples. Further, we would like to thank Sabine Kasten (AWI) for her support of the field campaign and sulfate measurements and particularly for her contribution to the scientific discussion. The divers and the crew of the Argentinean Antarctic Station Carlini (formerly: Jubany) and Dirk Mengedoht (AWI) are thanked for their logistic help.

This work was supported by the German Research Foundation (DFG) under grants AB 124/11-1, STA 936/5-1, and KA 2769/3-1 in the framework of priority program 1158 (Antarctic Research with Comparable Investigations in Arctic Sea Ice Areas) and is associated to the IMCOAST project. Dorothee Wilhelms-Dick acknowledges the DFG for financial support (GRK 717: Proxies in Earth History). We also thank the reviewer and the editor who greatly improved the manuscript.

References

- Abele, D., Atencio, A., Dick, D., Gonzalez, O., Kriews, M., Meyer, S., Philipp, E., Stoelting, I., 2008. Iron, copper and manganese discharge from glacial melting into Potter Cove and metal concentrations in *Laternula elliptica* shells. *Ber. Polar Meeresfor.* 571, 39–46.
- Ahn, I.Y., 1993. Enhanced particle flux through the biodeposition by the Antarctic suspension feeding bivalve *Laternula elliptica* in Marian Cove, King George Island. *J. Exp. Mar. Biol. Ecol.* 171, 75–90.
- Ahn, I.Y., Lee, S.H., Kim, K.T., Shim, J.E., Kim, D.Y., 1996. Baseline heavy metal concentrations in the Antarctic clam, *Laternula elliptica* in Maxwell Bay, King George Island, Antarctica. *Mar. Pollut. Bull.* 32, 592–598.
- Ahrland, S., 1975. Metal complexes present in seawater. In: Goldberg, E.D. (Ed.), *The Nature of Seawater*, Dahlem Workshop Report. Dahlem Konferenzen, Berlin, pp. 219–244.
- Anbar, A.D., 2004. Iron stable isotopes: beyond biosignatures. *Earth Planet. Sci. Lett.* 217, 223–236.
- Anbar, A.D., Rouxel, O., 2007. Metal stable isotopes in paleoceanography. *Annu. Rev. Earth Pl. Sc. Annual Reviews*, Palo Alto, pp. 717–746.
- Beard, B.L., Johnson, C.M., 2004. Inter-mineral Fe isotope variations in mantle-derived rocks and implications for the Fe geochemical cycle. *Geochim. Cosmochim. Acta* 68, 4727–4743.
- Beard, B.L., Johnson, C.M., Cox, L., Sun, H., Neelson, K.H., Aguilar, C., 1999. Iron isotope biosignatures. *Science* 285, 1889–1892.
- Beard, B.L., Johnson, C.M., Von Damm, K.L., Poulson, R.L., 2003. Iron isotope constraints on Fe cycling and mass balance in oxygenated earth oceans. *Geology* 31, 629–632.
- Bergquist, B.A., Boyle, E.A., 2006. Iron isotopes in the Amazon River system: weathering and transport signatures. *Earth Planet. Sci. Lett.* 248, 54–68.
- Berner, R.A., 1981. A new geochemical classification of sedimentary environments. *J. Sediment. Petrol.* 51, 359–365.
- Crosby, H.A., Roden, E.E., Johnson, C.M., Beard, B.L., 2007. The mechanisms of iron isotope fractionation produced during dissimilatory Fe(III) reduction by *Shewanella putrefaciens* and *Geobacter sulfurreducens*. *Geobiology* 5, 169–189.
- Curtosi, A., Pelletier, E., Vodopivec, C., St Louis, R., Mac Cormack, W.P., 2010. Presence and distribution of persistent toxic substances in sediments and marine organisms of Potter Cove, Antarctica. *Arch. Environ. Contam. Toxicol.* 59, 582–592.
- Deheyn, D.D., Gendreau, P., Baldwin, R.J., Latz, M.L., 2005. Evidence for enhanced bioavailability of trace elements in the marine ecosystem of Deception Island, a volcano in Antarctica. *Mar. Environ. Res.* 60, 1–33.
- Dickens, G., Koelling, M., Smith, D., Schnieders, L., Scientists, I.E., 2007. Rhizon sampling of pore waters on scientific drilling expeditions: an example from the IODP Expedition 302, Arctic Coring Expedition (ACEX). *Sci. Drill.* 4, 22–25.
- Froelich, P.N., Klinkhammer, G.P., Bender, M.L., Luedtke, N.A., Heath, G.R., Cullen, D., Dauphin, P., Hammond, D., Hartman, B., Maynard, V., 1979. Early oxidation of organic-matter in pelagic sediments of the eastern equatorial Atlantic – suboxic diagenesis. *Geochim. Cosmochim. Acta* 43, 1075–1090.
- George, S.G., Coombs, T.L., 1977. Effects of high stability iron-complexes on the kinetics of iron accumulation and excretion in *Mytilus edulis* (L.). *J. Exp. Mar. Biol. Ecol.* 28, 133–140.
- George, S.G., Pirie, B.J.S., Coombs, T.L., 1976. The kinetics of accumulation and excretion of ferric hydroxide in *Mytilus edulis* (L.) and its distribution in the tissues. *J. Exp. Mar. Biol. Ecol.* 23, 71–84.
- Gonzalez, P.M., Puntarulo, S., 2011. Iron and nitrosative metabolism in the Antarctic mollusc *Laternula elliptica*. *Comp. Biochem. Phys. C* 153, 243–250.
- Gonzalez, P.M., Abele, D., Puntarulo, S., 2010. Exposure to excess dissolved iron in vivo affects oxidative status in the bivalve *Mya arenaria*. *Comp. Biochem. Phys. C* 152, 167–174.
- Griscom, S.B., Fisher, N.S., 2004. Bioavailability of sediment-bound metals to marine bivalve molluscs: an overview. *Estuaries* 27, 826–838.
- Guelke, M., von Blanckenburg, F., 2007. Fractionation of stable iron isotopes in higher plants. *Environ. Sci. Technol.* 41, 1896–1901.
- Heinemann, A., Fietzke, J., Eisenhauer, A., Zumholz, K., 2008. Modification of Ca isotope and trace metal composition of the major matrices involved in shell formation of *Mytilus edulis*. *Geochem. Geophys. Geosyst.* 9, Q01006.
- Henkel, S., Kasten, S., Sala, H., Busso, A.S., Staubwasser, M., 2013. Effect of increased glacier melt on diagenetic Fe cycling in marine sediments at King George Island (Antarctica). *Goldschmidt 2013*, Florence, 25–30.08.2013.
- Homoky, W.B., Severmann, S., Mills, R.A., Statham, P.J., Fones, G.R., 2009. Pore-fluid Fe isotopes reflect the extent of benthic Fe redox recycling: evidence from continental shelf and deep-sea sediments. *Geology* 37, 751–754.
- Hotz, K., Walczyk, T., 2013. Natural iron isotopic composition of blood is an indicator of dietary iron absorption efficiency in humans. *J. Biol. Inorg. Chem.* 18, 1–7.

¹ The white-transparent hemolymph of the bivalve *L. elliptica* is free of hemoglobin.

- Hotz, K., Augsburg, H., Walczyk, T., 2011. Isotopic signatures of iron in body tissues as a potential biomarker for iron metabolism. *J. Anal. Atom. Spectrom.* 26, 1347–1353.
- Hotz, K., Krayenbuehl, P.-A., Walczyk, T., 2012. Mobilization of storage iron is reflected in the iron isotopic composition of blood in humans. *J. Biol. Inorg. Chem.* 17, 301–309.
- Husmann, G., 2013. The bivalve *Laternula elliptica*: physiological and molecular response to changing coastal Antarctic environments. Dissertation. Institut für Klinische Molekularbiologie, Kiel. <http://macau.uni-kiel.de/receive/dissertation_diss_00011510>.
- Husmann, G., Abele, D., Monien, D., Monien, P., Kriews, M., Philipp, E.E.R., 2012. The influence of sedimentation on metal accumulation and cellular oxidative stress markers in the Antarctic bivalve *Laternula elliptica*. *Estuar. Coast. Shelf S.* 111, 48–59.
- John, S.G., Mendez, J., Moffett, J., Adkins, J., 2012. The flux of iron and iron isotopes from San Pedro Basin sediments. *Geochim. Cosmochim. Acta* 93, 14–29.
- Kadar, E., Lowe, D.M., Sole, M., Fisher, A.S., Jha, A.N., Readman, J.W., Hutchinson, T.H., 2010. Uptake and biological responses to nano-Fe versus soluble FeCl₃ in excised mussel gills. *Anal. Bioanal. Chem.* 396, 657–666.
- Kasten, S., Zabel, M., Heuer, V., Hensen, C., 2004. Processes and signals of nonsteady-state diagenesis in deep-sea sediments and their pore waters. In: *The South Atlantic in the Late Quaternary*. Springer, Berlin Heidelberg, pp. 431–459.
- Kiczka, M., Wiederhold, J.G., Kraemer, S.M., Bourdon, B., Kretzschmar, R., 2010. Iron isotope fractionation during Fe uptake and translocation in alpine plants. *Environ. Sci. Technol.* 44, 6144–6150.
- King, P., Broderip, W., 1832. Description of the Cirripedia, Conchifera and Mollusca in a collection formed by the officers of HMS Adventure and Beagle employed between the years 1826 and 1830 in surveying the southern coasts of South America, including the straits of Magalhaens and the coast of Tierra del Fuego. *Zool. J.* 5, 332–349.
- Krayenbuehl, P.A., Walczyk, T., Schoenberg, R., von Blanckenburg, F., Schulthess, G., 2005. Hereditary hemochromatosis is reflected in the iron isotope composition of blood. *Blood* 105, 3812–3816.
- Lohan, M.C., Statham, P.J., Peck, L., 2001. Trace metals in the Antarctic soft-shelled clam *Laternula elliptica*: implications for metal pollution from Antarctic research stations. *Polar Biol.* 24, 808–817.
- Millero, F.J., Yao, W., Aicher, J., 1995. The speciation of Fe(II) and Fe(III) in natural waters. *Mar. Chem.* 50, 21–39.
- Monien, D., Monien, P., Bruenjes, R.M., Widmer, T., Schnetger, B., Brumsack, H.-J., 2013. Sedimentary regimes at Potter Cove, King George Island, maritime Antarctica – from source to sink. *European Geosciences Union General Assembly 2013. Geophys. Res. Abstracts* 15, 7454.
- Nigro, M., Regoli, F., Rocchi, R., Orlando, E., 1997. Heavy metals in Antarctic molluscs. In: Battaglia, B. (Ed.), *Antarctic Communities Species and Survival*. Cambridge University Press, Cambridge, pp. 409–412.
- Norkko, A., Thrush, S.F., Cummings, V.J., Gibbs, M.M., Andrew, N.L., Norkko, J., Schwarz, A.M., 2007. Trophic structure of coastal antarctic food webs associated with changes in sea ice and food supply. *Ecology* 88, 2810–2820.
- Ohno, T., Shinohara, A., Kohge, I., Chiba, M., Hirata, T., 2004. Isotopic analysis of Fe in human red blood cells by multiple collector-ICP-mass spectrometry. *Anal. Sci.* 20, 617–621.
- Poigner, H., 2013. Iron and manganese in Antarctic bivalves: Indicators of change in near-shore biogeochemistry? Dissertation, Universität Oldenburg. <<http://oops.uni-oldenburg.de/1823/>>.
- Poigner, H., Monien, P., Monien, D., Kriews, M., Brumsack, H.J., Wilhelms-Dick, D., Abele, D., 2013a. Characterization of metals in hemolymph and tissues of the Antarctic bivalve *Laternula elliptica*. <www.pangaea.de>, <http://dx.doi.org/10.1594/PANGAEA.776600>.
- Poigner, H., Monien, P., Monien, D., Kriews, M., Brumsack, H.J., Wilhelms-Dick, D., Abele, D., 2013b. Influence of the pore water geochemistry on Fe and Mn assimilation in *Laternula elliptica* at King George Island (Antarctica). *Estuar. Coast. Shelf S.* 135, 285–295.
- Poulton, S.W., Canfield, D.E., 2005. Development of a sequential extraction procedure for iron: implications for iron partitioning in continentally derived particulates. *Chem. Geol.* 214, 209–221.
- R Development Core Team, 2010. R: A Language and Environment for Statistical Computing. R Foundation for Statistical Computing, Vienna, Austria.
- Rainbow, P.S., 2002. Trace metal concentrations in aquatic invertebrates: why and so what? *Environ. Pollut.* 120, 497–507.
- Raiswell, R., Canfield, D.E., 2012. The iron biogeochemical cycle past and present. *Geochem. Perspect.* 1, 1–220.
- Raiswell, R., Tranter, M., Benning, L.G., Siebert, M., De'ath, R., Hybrechts, P., Payne, T., 2006. Contributions from glacially derived sediment to the global iron (oxyhydr)oxide cycle: implications for iron delivery to the oceans. *Geochim. Cosmochim. Acta* 70, 2765–2780.
- Raiswell, R., Benning, L.G., Tranter, M., Tulaczyk, S., 2008. Bioavailable iron in the Southern Ocean: the significance of the iceberg conveyor belt. *Geochem. Trans.* 9, 7.
- Rey, J., Somoza, L., Martinezfrias, J., 1995. Tectonic, volcanic, and hydrothermal event sequence on Deception Island (Antarctica). *Geo-Mar. Lett.* 15, 1–8.
- Schoenberg, R., von Blanckenburg, F., 2005. An assessment of the accuracy of stable Fe isotope ratio measurements on samples with organic and inorganic matrices by high-resolution multicollector ICP-MS. *Int. J. Mass Spectrom.* 242, 257–272.
- Seeberg-Elverfeldt, J., Schlueter, M., Feseker, T., Kolling, M., 2005. Rhizon sampling of porewaters near the sediment-water interface of aquatic systems. *Limnol. Oceanogr.-Meth.* 3, 361–371.
- Severmann, S., Johnson, C.M., Beard, B.L., McManus, J., 2006. The effect of early diagenesis on the Fe isotope compositions of porewaters and authigenic minerals in continental margin sediments. *Geochim. Cosmochim. Acta* 70, 2006–2022.
- Severmann, S., McManus, J., Berelson, W.M., Hammond, D.E., 2010. The continental shelf benthic iron flux and its isotope composition. *Geochim. Cosmochim. Acta* 74, 3984–4004.
- Simkiss, K., Mason, A.Z., 1983. Metal ions: metabolic and toxic effects. In: Hochachka, P.W., Wilbur, K.M. (Eds.), *The Mollusca: Environmental Biochemistry and Physiology*. Academic Press Inc., New York, pp. 101–164.
- Simkiss, K., Taylor, M., 1981. Cellular mechanisms of metal ion detoxification and some new indices of pollution. *Aquat. Toxicol.* 1, 279–290.
- Slomp, C.P., Malschaert, J.F.P., Lohse, L., van Raaphorst, W., 1997. Iron and manganese cycling in different sedimentary environments on the North Sea continental margin. *Cont. Shelf Res.* 17, 1083–1117.
- Staubwasser, M., von Blanckenburg, F., Schoenberg, R., 2006. Iron isotopes in the early marine diagenetic iron cycle. *Geology* 34, 629–632.
- Staubwasser, M., Schoenberg, R., von Blanckenburg, F., Krueger, S., Pohl, C., 2013. Isotope fractionation between dissolved and suspended particulate Fe in the oxic and anoxic water column of the Baltic Sea. *Biogeosciences* 10, 233–245.
- Taylor, P.D.P., Maek, R., De Bièvre, P., 1992. Determination of the absolute isotopic composition and atomic weight of a reference sample of natural iron. *Int. J. Mass Spectrom. Ion Process.* 121, 111–125.
- Waite, T.D., 2001. Thermodynamics of the iron system in seawater. In: Turner, D.R., Hunter, K.A. (Eds.), *The Biogeochemistry of Iron in Seawater*. John Wiley & Sons Ltd., West Sussex, England, pp. 291–342.
- Walczyk, T., von Blanckenburg, F., 2002. Natural iron isotope variations in human blood. *Science* 295, 2065–2066.
- Walczyk, T., von Blanckenburg, F., 2005. Deciphering the iron isotope message of the human body. *Int. J. Mass Spectrom.* 242, 117–134.
- Zhu, X.K., Guo, Y., Williams, R.J.P., O'Nions, R.K., Matthews, A., Belshaw, N.S., Canters, G.W., de Waal, E.C., Weser, U., Burgess, B.K., Salvato, B., 2002. Mass fractionation processes of transition metal isotopes. *Earth Planet. Sci. Lett.* 200, 47–62.